

Tautomeric Transitions in DNA

V.L. Golo and Yu.S. Volkov

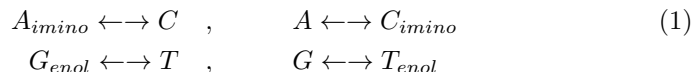
Department of Mechanics and Mathematics
Moscow State University
Moscow 119899, Russia

Abstract

We study the tautomeric transitions in base pairs of DNA considering elastic properties of DNA as classical and tunneling of protons as quantum, and show that the dynamics of the transitions admits of soliton like solutions whose shape and size strongly depend on the structure of the double helix. In particular, we have found that the set of discrete breathers can be drastically modified by the interplay of the torsional and elastic constants. Our results may have a bearing upon substitution mutagenesis within the framework of Watson-Crick's approach, and in this respect the breather soliton could describe conformations corresponding to point mutations. The numerical simulation of soliton dynamics suggests that an initial distribution of base pairs with low probability of mutation per pair but of a sufficiently large number of base pairs involved, could move and gather around a site so as to form a set of base pairs with high probability of mutation, for a period of time approximately $1 \mu\text{sec}$. We suggest that the irradiation of DNA at frequencies of the proton tunneling, that is in infra-red region, could cause mutations.

1. Introduction

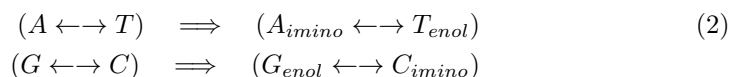
According to the Watson-Crick hypothesis, [1], the life is built around a symmetrical figure, the double helix of the DNA molecule (see Fig.1), which comprises the two strands linked together by purine-pyrimidine base-pairs of adenine-thymine (AT) and guanine-cytosine (GC), the four chemicals A,T,G,C existing in various isomeric forms, or tautomers, that may change into one another (see Fig.2). Under ordinary conditions the equilibrium shifts towards the amino-form for adenine and guanine, and the keto-form for thymine and cytosine. But the imino-form for the adenine and cytosine, and the enol-form for guanine and thymine are also possible, even though rare; in fact, they correspond to concentrations of 10^{-4} to 10^{-5} moles/liter, [2]. To see the implications wrought by the tautomeric transitions let us recall that the sequence of base-pairs constitutes the genetic information of cell. It should be noted that adenine will pair only with thymine by two hydrogen bonds, and guanine with cytosine with three hydrogen bonds, so that exact copies of the DNA are produced during the replication (see Fig.3). But the complementarity between the bases is completely changed if a tautomeric transition takes place; in fact, owing to the structure of hydrogen bonds other combinations become possible (see Fig.4),



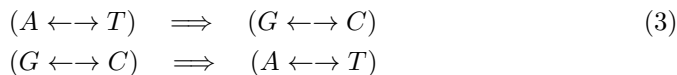
in contrast to the usual and stable ones



Another opportunity for generating "unnatural" pairs arises from the tunneling of protons in hydrogen bonds (see Fig.5), which results in the formation of the pairs



During the replication, tautomeric transition driven by the proton tunneling in conjunction with the complementarity according to (2) may lead to the change of base-pairs



and result in loss, or corruption, of genetic information, i.e. mutations, [3], [4]. The specific case given by the diagram (3) is called transition mutations; it has the property of being reversible, i.e. able to go back to the wildlife type.

The arguments given above constitute the main points of the theory of spontaneous mutations suggested by Crick and Watson, [3], [5], [6]. It is based on

the assumption that the transitory tautomeric shifts of base-pairs may occur during the replication, i.e. when two molecules of DNA are formed from a paired molecule, so that the double-stranded molecule is split into two single strands, each of which controls the synthesis of a new strand complimentary to itself with the help of the special enzyme called DNA polymerase. It has been realized that the latter plays an active role in the selection of bases at replication, [7], so that it may affect the mutation rates. Thus, tautomeric transitions are not a unique cause of mutation; the situation is more subtle, and many questions, of quite a classical nature, wait their solutions. Nonetheless, the original idea of Watson and Crick still conserves its appeal, and even more so as its new links with other phenomena related to the mutagenesis are brought to light (see [8], [9]). So, Robinson et al, [9] report that the enol tautomer of *iG*, that is 2'-deoxyisogine, may form at physiological temperature (37°) and pair with thymine in a Watson-Crick geometry (see Fig.14); thus, *iG* present as the nucleoside, results in the formation of incorrect base-pairs during in vitro replication, [10],[11], [12],[13],[15]. Robinson et al, [9], suggests that *iG* · *T* pairing may have a bearing on mutagenesis in vivo involving tautomers of the common nucleobases. On the other hand, Fresco et al, [14], have found that the imino tautomer *HO⁵dCyt* may serve as an example of an unfavored base tautomer making for substituting mutagenesis.

Mutations within the framework of the Crick-Watson model of DNA and in conjunction with the concept of tautomeric transition, have been drawing attention, beginning from the early fifties, [1], [3], [6], to the present time, and involved the use of condensed matter theory. So, one of the first papers in this direction was published by Geracitano and Persico, [16], who suggested that there should be expected a collective behavior of codons, resembling that taking place in hydrogen-bonded ferroelectric crystals.

In this paper we intend to look after the interplay between tautomeric transitions in base-pairs and elastic properties of the double helix. Since the π -electrons of the tautomeric rings of the nucleotides have direct bearing on the interaction of the plates of adjacent base-pairs, [17], [18], we suggest that the tautomeric transition of base-pairs should substantially influence the distribution of delocalized electrons of the nucleotides, i.e. the π -electrons, and result in deformation of the elastic system of DNA. It is worth noting that tautomeric transitions may occur in several base pairs, not necessary adjacent, at a time, and their dynamics is determined by the proton tunneling. For one thing the latter is determined by the electrostatic interaction, i.e. the dipole forces, between the protons belonging to adjacent base-pairs, and for another by the elastic system of the DNA molecule, which should play a role like that of the crystalline lattice of the polaron theory. The situation is similar to that considered in the Davydov theory for the α -helix of proteins, [19]. To put these arguments in a more quantitative form we begin by recalling certain facts

concerning the elastic properties of DNA.

2. The torsional modes of DNA

From the mechanical point of view, the DNA molecule is a very unusual object. For one thing one can visualize it as an elastic rod and consider it within the framework of the mechanics of continuous media, thus obtaining reasonable agreement with experiment, [20], for another it is often necessary to study DNA as a discrete system similar to crystalline lattice. In the present paper we have to deal with an intermediate situation for which a cautious use of the methods of continuous media is justifiable. In fact, as far as the transport of torsional stress (torque) along DNA is concerned, its estimates obtained by various means diverge widely. The numerical values derived with the help of the theory of continuous media, [22], are of the order $\tau \propto 10^{-17} \text{ dyne} \cdot \text{cm}$, [20], [21], whereas there is the experimental evidence, [23], that it can attain the value of $\tau \propto 10^{-13} \text{ dyne} \cdot \text{cm}$. Philip Nelson, [20], suggested that these deviations could be due to small bends in the helix backbone, so that one may assume

$$\tau \propto 10^{-17} \div 10^{-13} \text{ dyne} \cdot \text{cm}$$

As was mentioned above, the interplay between the torsional stress due to the relative motion of the base-pairs and the proton tunneling is very important. We shall use the approach worked out in [24] and [26] to describe the elastic properties of the double helix. Thus, the double helix is considered as a one-dimensional lattice of vectors \vec{y}_n describing the mutual position of the two strands at sites corresponding to the base-pair of index n. It is important that the system has a twisted ground state characterized by the twist vector $\vec{\Omega}$, so that the elastic energy of the molecule can be cast in the form

$$H_{tor} = \sum_{i=1}^N \frac{1}{2} M (\partial_t \vec{y}_i)^2 + \sum_{i=1}^N \frac{1}{2} K (\nabla \vec{y}_i)^2 + \sum_{i=1}^N \frac{1}{2} \epsilon \vec{y}_i^2 \quad (4)$$

where the first term is the kinetic energy, the second one the elastic torsional energy and the last one corresponds to the separation of the two strands. The covariant derivative that accommodates the torsion of the molecule, reads

$$\nabla \vec{y}_i = \frac{1}{a} \left(\vec{y}_{i+1} - \vec{y}_i + \vec{\Omega} \times \vec{y}_i \right)$$

Here a is the spacing between the adjacent nucleotides, M is the mass of base-pair. It should be noted that we are considering a very simplified model and assume that all sites, corresponding to base-pairs are identical. The subtle question is the value of the elastic constant K ; obviously enough it has a direct

bearing on the torque τ mentioned above, and therefore its estimate may read

$$K \propto 10^{-13} \div 10^{-17} \text{ erg}$$

It should be noted that the calculations within the framework of molecular dynamics, (see paper [27] and references therein), give the upper value for K , i.e. close to $10^{-12} \div 10^{-13}$ erg. For the sake of simplicity, in this paper we shall assume that the torsion vector $\vec{\Omega}$ is always parallel to the axis Oz, that is

$$\vec{\Omega} = (0, 0, \Omega)$$

and the vectors \vec{y}_n describe only transversal motions, that is $y_n^3 = 0$.

As was mentioned above the tautomeric transitions are driven by the proton tunneling, and therefore we shall describe them quantum mechanically, that is the stable amino/keto form corresponding to the ground state of proton, and the unstable imino/enol one to the excited state, [25]. In accord with the qualitative character of our approach we neglect the fact that the tautomeric transitions in question involve the tunneling of more than one proton, and assign only one proton to each site of the lattice.

It is important that there are few hydrogen bonds in which the protons are transferred towards the imino/keto groups, or if one uses the concept of the two-level system, the excited states. Therefore, one can consider the system as being close to equilibrium, or only weakly excited. This suggestion is very important for what follows.

We shall describe the states of a base-pair at site n with the Bose operators b_n^+ , b_n that verify the usual conditions

$$[b_n, b_m^+] = b_n b_m^+ \quad - \quad b_m^+ b_n = \delta_{nm}, \quad [b_n, b_m] = [b_n^+, b_m^+] = 0$$

so that the energy of the protons, neglecting the interaction with the elastic degrees of freedom, reads, [25]

$$H_P = \sum_n E_o b_n^+ b_n \quad + \quad \kappa \sum_n (b_n^+ b_{n+1} + b_{n+1}^+ b_n)$$

Here E_o is the energy of the tautomeric shift; its estimates depend on the choice of nucleotide and according to quantum chemistry calculations vary within the range of $2 \div 10$ Kcal, (see [2] and references therein). The constant κ could be ascribed to dipole interactions between adjacent sites, similarly to Davydov's theory, [19]. Presently, there are no reliable estimates of its value (see below); by analogy with the Davydov theory one may assume that it should correspond to the characteristic frequency of proton, or tautomeric, excitation of the order 10^{11} , or less. This figure is generally accepted (see below).

The central point of the model introduced in [25] is the interaction between the elastic degrees of freedom of DNA and the tautomeric transitions, or the proton tunneling in nucleotides; it reads

$$H_I = -\lambda \sum_n \left(\nabla \vec{y}_n \cdot \vec{h}_n \right) b_n^+ b_n$$

An argument in favor of this choice is that it takes into account the deformation of positions of adjacent base-pairs and thus its influence on the π -electrons of the bases, and therefore, the tautomeric transitions, or the related excitations of protons. According to the theory of [18], the interaction could be appreciable. Thus, one may suggest that the interaction term could be larger than the tunneling term in the equation for H_P given above.

Concluding we may state that the total energy within the framework of the model introduced in [25] has the form

$$H_{total} = H_{tor} + H_P + H_I$$

The conditions discussed above are exactly those used for Davydov's theory, [19]. Let us recall its main points. It is assumed that the state of the system can be described by a trial function that has the form

$$|\mathcal{D}\rangle = \sum_n A_n(t) \cdot b_n^+ |0\rangle \quad (5)$$

where $|0\rangle$ is the vector designating the ground state of the system, that is all the base-pairs, or the protons in the hydrogen bonds, being in the ground state. The amplitudes $A_n(t)$ are subject to the constraint

$$\sum_n |A_n(t)|^2 = 1 \quad (6)$$

At this point it should be noted the vectors \vec{y}_n describe the dynamics of base-pairs, that is relatively massive objects, and therefore one may consider them as classical fields, [25], [26]. We can derive the size of characteristic frequencies for \vec{y}_n from expression (4) of the elastic energy. In fact, the mass M is that of the base-pair, that is of the order 500 Dalton, and K is of the same order of magnitude as τ . Hence, we get the characteristic velocity v for the \vec{y} modes

$$v \propto \sqrt{\frac{K}{M}}$$

Interesting numerical values for the velocity v follow from the equation indicated above and the rough estimates for τ or K we have mentioned. Indeed, for $K \propto 10^{-17} \text{ dyn} \cdot \text{cm}$ or less we obtain

$$v \propto 10^2 \text{ cm/sec}$$

For wavelengths of a few tens of Å it gives the characteristic torsion or phonon frequencies of the order

$$\omega_y \propto 10^8 \div 10^9 \text{ Hz}$$

On the other hand, if we use the values for K provided by the molecular dynamics simulations, [27], we get the velocity of excitations of the order 1000 m/sec , and $\omega_y \propto 10^{11} \div 10^{12} \text{ Hz}$, as for ordinary condensed media. It is instructive to compare the values of ω_y with the transition frequencies for tautomeric reactions inside the nucleotides,

$$\omega_P = \frac{\kappa}{2\pi\hbar}$$

The estimates for the latter differ considerably, [32], [33]

$$\omega_P \propto 10^6 \div 10^{11} \text{ Hz}$$

The lowest estimate, 10^6 Hz appears to be not unreasonable (V. Benderskii, and J.L.Leroy, personal communications).

The relative sizes of ω_P and ω_y are important for choosing the right approximation for the model. In fact, if we are at the lowest end of the spectra ω_P , then according to the estimate for ω_y obtained above the characteristic times for the acoustic modes are at least by an order of magnitude smaller than for the protons. In this case, we may suggest that the elastic system should follow the motion of the protons in hydrogen bonds, adjusting itself to it, so that the situation is similar to that of the Born-Oppenheimer approximation in the atomic theory.

Thus, we assume, as in paper [25], that the adiabatic approximation is valid, and therefore we may neglect the kinetic energy of the elastic system and take into account only its potential energy generated by the field \vec{y}_n . Then we are in a position to apply Davydov's method, [19], that is to calculate the mean value

$$U_{eff} = \langle \mathcal{D} | H_{tor} + H_I | \mathcal{D} \rangle$$

find the minimum, $\vec{y}_n^{(o)}$ of U_{eff} with respect to \vec{y}_n , substitute it into the equation for the total energy H_{total} so as to get the effective Davydov hamiltonian \mathcal{H}_D , which depends only on the operator variables b_n^+ , b_n , the classical variables \vec{y}_n having disappeared through the minimization. Thus, we obtain an equation that has the form of the Schrödinger one

$$i\hbar \frac{\partial}{\partial t} | \mathcal{D} \rangle = \mathcal{H}_D | \mathcal{D} \rangle \quad (7)$$

and in which the wave function $|\mathcal{D}\rangle$ should be of the form (5). The assumption that the excited states correspond to the set of two-level systems is accommodated by the requirement that the operators b_n^+ are allowed only in the first power. It results in a system of equations, called the Davydov equations, for the amplitudes A_n , which one obtains on equating the coefficients at b_n^+ on both sides of (7), (see [19] for the details). All the necessary calculation for the model of the DNA we employ, had been done in [25], on which the present paper relies.

The Davydov hamiltonian for our problem reads

$$\begin{aligned}
H_D = & \sum_n E_0 b_n^+ b_n - \sum_n \kappa (b_{n+1}^+ b_n + b_n^+ b_{n+1}) \\
& - \frac{\lambda^2}{k} \sum_n |A_n|^4 - \frac{\lambda^2}{k} \sum_n |A_n|^2 b_n^+ b_n \\
& + \frac{\lambda^2}{2k} \frac{\epsilon a^2}{k \Omega^2} \sum_{m,n} \cos^{|m-n|} \phi \cdot \cos [(m-n)(\phi - \alpha)] |A_m|^2 |A_n|^2 \\
& + \frac{\lambda^2}{2k} \frac{\epsilon a^2}{k \Omega^2} \sum_{m,n} \cos^{|m-n|} \phi \cdot \cos [(m-n)(\phi - \alpha)] |A_n|^2 b_m^+ b_m
\end{aligned}$$

and the equation for the amplitudes A_n

$$\begin{aligned}
i\hbar \frac{\partial}{\partial t} A_n = & E_0 A_n - \kappa (A_{n+1} + A_{n-1}) \\
& - \frac{\lambda^2}{k} |A_n|^2 A_n - \frac{\lambda^2}{k} \left(\sum_m |A_m|^4 \right) A_n \\
& + \frac{\lambda^2}{k} \frac{\epsilon a^2}{k \Omega^2} \left(\sum_{m_1, m_2} \cos^{|m_1 - m_2|} \phi \cdot \cos [(m_1 - m_2)(\phi - \alpha)] |A_{m_1}|^2 |A_{m_2}|^2 \right) A_n \\
& + \frac{\lambda^2}{k} \frac{\epsilon a^2}{k \Omega^2} \left(\sum_m \cos^{|m-n|} \phi \cdot \cos [(m-n)(\phi - \alpha)] |A_m|^2 \right) A_n
\end{aligned}$$

see [25] for the details.

3. The numerical simulation

We introduce the reduced variables B_n according to the equation

$$A_n = e^{-\frac{i}{\hbar} E_0 t} B_n(t)$$

and cast the equation for A_n in the form

$$\begin{aligned} i\hbar \frac{\partial}{\partial t} B_n &= -\kappa(B_{n+1} + B_{n-1}) - \frac{\lambda^2}{k} |B_n|^2 B_n \\ &\quad - \frac{\lambda^2}{k} \left(\sum_m |B_m|^4 \right) B_n \\ &\quad + \frac{\lambda^2}{k} \frac{\epsilon a^2}{k \Omega^2} \left(\sum_{m_1, m_2} \cos^{|m_1 - m_2|} \phi |B_{m_1}|^2 |B_{m_2}|^2 \right) B_n \\ &\quad + \frac{\lambda^2}{k} \frac{\epsilon a^2}{k \Omega^2} \left(\sum_m \cos^{|m-n|} \phi |B_m|^2 \right) B_n \end{aligned} \quad (8)$$

Here

$$\phi = \arctan \Omega$$

The non-local terms are a consequence of the structure of double-helix, often neglected in considering the dynamics of DNA, [28].

Introduce the characteristic frequencies

$$\omega_P = \frac{\kappa}{2\pi\hbar}, \quad \omega_T = \frac{\lambda}{2\pi\hbar}, \quad \omega_{tor} = \frac{K}{2\pi\hbar} \quad (9)$$

and the dimensionless time

$$\Upsilon = t \cdot \omega_P$$

It should be noted that the frequencies ω_y and ω_{tor} are not identical, $\omega_y \neq \omega_{tor}$. Then the Davydov equation takes the form

$$\begin{aligned} i \frac{\partial}{\partial \Upsilon} B_n &= -(B_{n+1} + B_{n-1}) - W |B_n|^2 B_n \\ &\quad - W \left(\sum_m |B_m|^4 \right) B_n \\ &\quad + W \Lambda \left(\sum_{m_1, m_2} \cos^{|m_1 - m_2|} \phi |B_{m_1}|^2 |B_{m_2}|^2 \right) B_n \\ &\quad + W \Lambda \left(\sum_m \cos^{|m-n|} \phi |B_m|^2 \right) B_n \end{aligned} \quad (10)$$

in which

$$W = \frac{\omega_T^2}{\omega_P \cdot \omega_{tor}} \quad (11)$$

$$\Lambda = \frac{\epsilon a^2}{k \cdot \Omega^2} \quad (12)$$

Now we aim at making the numerical simulation of equation (10) for various values of the parameters W , Λ , looking for solutions of the soliton type. We use the term soliton in a sense close to that used by applied scientists, i.e. a solution different from zero in a finite region of space, whose *size we shall call the size of soliton* and preserving its shape for very long periods of time. For some values of W , Λ it has the form identical to the usual one, i.e. corresponding to the non-linear Schrödinger equation, but generally our solitons are different. The standard definition suggests that it be of the form

$$Y(x, t) = e^{i(qx - \nu t)} \psi(x - \nu t) \quad (13)$$

in which ψ is a real function. It is by no means clear that solutions that we suppose to be solitons, always have the form given by equation (13).

The parameter Λ is a quantitative characteristic that enables us to take into account the structure of the double helix, and also the relative size of the torsional and deformation energies. In fact, Λ determines the magnitude of the nonlocal terms in equation (10), and in this respect it is worthwhile to note that for certain values of Λ and W we have not been able to find soliton solutions, e.g. $\Lambda = 0.2$ and $W = 2$, at least for physically reasonable sizes of solitons, i.e. less than 100 base pairs. But it is important that generally the condition $\Lambda \neq 0$ does not forbid the existence of solitons, and its influence only results in the size of soliton becoming larger, which is quite natural, for Λ represents non-local terms in equation (10). The general case of soliton with Λ not equal to zero, even though small, is illustrated in Fig.8.

To illustrate the general situation let us consider the two special cases (for the details of calculation see Appendix).

1. Stationary solutions in the sense that the absolute value, $|B_n(t)|$ does not depend on time. For the usual solitons given by (10) this requirement means that the velocity $\nu = 0$. The typical case is illustrated in Fig.9, for $W = 10$ and $\Lambda = 0.5$. The half-width of soliton is equal one spacing between base-pairs, that is the solution is extremely narrow, and according to our main hypothesis it must correspond to the tautomeric transition of a base-pair. The very interesting case is illustrated in Fig.10, $W = 5$ and $\Lambda = 0.5$. There is a central peak of half-width $1.5 \cdot a$ which stands still, and two symmetrical wave packets, moving in opposite outward directions. The distance traveled by these wave packets during 0.018 msec is equal to 33 base pairs.

2. The usual solitons given by (10). The half-width of these solitons may be several tens of base-pair spacings, and thus they could correspond to tautomeric transitions taking place in adjacent base-pairs. The typical cases are illustrated in Fig.11, 12. The distance traveled by soliton in Fig.11 during 0.53 msec is equal to 707 base pairs, and the distance traveled by soliton in Fig.12 during 0.577 msec is equal to 491 base pairs. It is interesting to note that these solitons

move, even though slowly. Hence, one might suggest the picture of tautomeric transitions moving along the DNA-molecule.

Both types of solutions indicated above are stable with respect to perturbation of W and Λ .

Perhaps, the most characteristic feature of discrete non-linear Schrödinger equation is solutions that periodically oscillate in time and decay exponentially in space, or breathers, [31]. From a purely qualitative point of view the existence of breathers can be inferred from a truncated version of equation (10). Let us neglect all the terms on its RHS except the first two, that is consider

$$i\hbar \frac{\partial B_n}{\partial t} = -(B_{n+1} + B_{n-1}) - W|B_n|^2 B_n$$

and look for B_n such that

$$B_n = e^{i\nu t} a_n$$

a_n being real. Next, cast the equation for a_n in the form

$$-(a_{n+1} - 2a_n + a_{n-1}) - [W a_n^3 + (2 - \epsilon)] a_n = 0$$

Suppose that the soliton we are looking for is large enough so that we may change the expression $a_{n+1} - 2a_n + a_{n-1}$ for the second derivative. Thus we obtain the equation

$$a'' + [W a^3 + (2 - \epsilon)] a = 0$$

or the conservation law for one dimensional motion with the effective potential

$$V = \frac{2 - \epsilon}{2} a^2 + \frac{W}{4} a^4$$

The soliton solution exists for $\epsilon \geq 2$, and its size tends to infinity as $\epsilon \rightarrow 2$. On the other hand for large W we may expect thin solitons.

The key point is that the nonlocal terms generated by the double helix bring serious modifications to the picture given above.

We may infer from the examples given above that the dimensionless constants W and Λ play a crucial role in determining the form of solitons for equation (10). The general situation to the effect is illustrated in Figs.16 (a)-(b), in which the horizontal axis corresponds to values of ν , that is the soliton frequency measured in units of ω_P . It should be noted that ν is well defined for solitons of the form given by equation (13); in contrast, there is a fine structure in the frequency spectrum of breathers, [31], so that ν turns out to be only a rough characteristic. In fact, in Figs.16 (a)-(b) the values of ν are determined to within about one hundredth of ω_P . As is shown in Figs.16 (a)-(c) for $\Lambda = 0, 0.1, 0.15$, respectfully, the set of W and ν , for which there are solitons or breathers, consists of a line corresponding to breathers, and a region, or domain, for moving solitons. The line serves also as a right border for the region of moving solitons. The lower border of the soliton region is not strictly defined owing to the fact that there are solitons for values of W and ν lower than the borders but of sizes greater than 100 base pairs, that is outside the physical context of our problem. The upper left part of the border is determined by solitons turning out to be unstable for values of W and ν beyond the boundary. We see that the soliton region is decreasing as Λ grows, and for $\Lambda = 0.2$, Fig.16 (d), there are only breathers, at least under the constraint of their size being less than 100 base pairs. It is worth noting that the equation (10) derived in [25] is valid only for small Λ .

We would like to draw attention to a class of solutions that are not solitons, but nonetheless may have a bearing upon the dynamics of tautomeric transitions. A solution of the type is illustrated in fig.13. It is characterized by an initial set of amplitudes $B_n(t)$ which is a broad distribution of the size of 80 base-pair spacings; after the period of time 0.017 msec, it focuses itself on a narrow peak of half-width of one spacing. The peak exists for the brief period of time 0.002 msec, and next breaks down into a broad distribution again, i.e. a kind of partial self focusing is taking place. Thus, there may exist low probability tautomeric transitions distributed over wide areas of the molecule, and which may collapse into a small region of the molecule, and stay there for a period of time, brief but perhaps sufficient to cause mutation.

Finally, we wish to tell that our simulations used the standard numerical methods, i.e. the trapezoid, the Adams-Boshoft and the Adams-Moulton of the fourth order, the algorithm for stiff systems. An important test has been the conservation of the normalization condition

$$\sum_n |B_n(t)|^2 = 1 \tag{14}$$

For testing the precision of our algorithms we have also used calculations backwards in time.

4. Conclusions

As was shown above the dynamics of tautomeric transitions in DNA depend on elastic properties of the latter and proton tunneling in base pairs; W and Λ serving as indicators for possible regimes. Our numerical simulation suggests that the interesting tautomeric dynamics may happen for $W \geq 1$. This allows for sufficiently wide range of material constants of DNA so as to hope the phenomenon's taking place. The second constant, Λ , provides a quantitative characteristic for the part played by the double helix; it can totally modify the structure of solitons corresponding to tautomeric transitions.

Depending on the value of W one may expect the existence of two quite different kinds of soliton dynamics. The first one belongs to solitons that move at velocity of several 0.01 cm/sec , have a size of several tens of base-pairs, and the second of stationary solutions, or breathers, that have a form of peaks over a few base-pairs. We may suggest that the second type of solutions correspond to point mutations, whereas the first one may describe tautomeric transition moving along the chain of double helix. According to the Crick-Watson approach, there may happen mutations related to the transition. Thus, one may suggest that an action imposed on a set of nucleotide in a region of the molecule might generate mutations in a different region owing to the motion of excitations corresponding to proton tunneling.

It is alleged to be known that by substituting the "artificial" nucleotides instead of the natural ones, e.g. brom-uracil for thymine (see Fig.6,7), one can increase dramatically the rate of mutations; this could be due to the increase of tautomeric transitions inside base-pairs. At any rate, it is worthwhile to study the interplay between the rate of such transitions and mutations. Within the context of the present paper, artificial DNA of this kind could ease the stringent constraints imposed on W , as was indicated above.

It is worth noting that the "focusing" of solutions (see Fig.13) may have a very important bearing on mutations. In fact, it amounts to the possibility of a weak external influence generating a low amplitude distribution of mutation sites that would focus itself later on a high amplitude distribution concentrated in a different region of the molecule. Thus, one may expect generating mutations by low intensity agents distributed in a region of the molecule, or to put it the other way round, acting on a set of codons different from those that suffer the actual mutation.

Finally we would like to point out that the irradiation with electro-magnetic waves at frequencies of the proton tunneling in hydrogen bonds may result in tautomeric transitions of nucleotides, and, according to the arguments given in this paper, mutations. This circumstance could be used for experimental verification of our model.

The authors are thankful to V. Benderskii and R.Lavery for interesting discussion.

Appendix - Radiation Filtering (RF) Algorithm

The method used in this paper for constructing soliton solutions is based on the following heuristic argument. Suppose we have a solution that is close to a soliton, then we may visualize it as a central peak that radiates waves of small amplitude (see Fig.10), during the evolution in time. In case of soliton proper, the radiation is absent, so that the radiation is a specific feature that gives a measure of not being a soliton, so that the difference between the central peak and the soliton is carried away by the radiation. Hence, the soliton solution may be obtained by annihilating the radiation through the use of an appropriate filter (see Fig. 14).

The actual algorithm runs as follows: Take the parameter of cutoff, Π , which determines the level of noise to be absorbed, and the parameter *Err* for estimating the precision.

1. Let us take a trial set of amplitudes \tilde{B}_n ($n = 0 \dots N - 1$), that is the real and the imaginary parts $\text{Re } \tilde{B}_n$, $\text{Im } \tilde{B}_n$ and the absolute values $|\tilde{B}_n|$.
2. Consider the evolution of \tilde{B}_n described by equation (10) for the initial values given by the set \tilde{B}_n , that is $B_n(t = 0) = \tilde{B}_n$ ($n = 0 \dots N - 1$) for the time interval Δt , and take the set of amplitudes $\hat{B}_n = B_n(t = \Delta t)$.
3. Consider the set of absolute values $|\hat{B}_n|$, and find the index M for the maximum value, B_M , of $|\hat{B}_n|$ ($n = 0 \dots N - 1$).
4. Find the indices L and R such that $|\hat{B}_L|$ and $|\hat{B}_R|$ are both local minima of the set $|\hat{B}_n|$, and the constraints
 - (i) $|\hat{B}_L| < \Pi$ and $|\hat{B}_R| < \Pi$,
 - (ii) $L < M < R$,
 - (iii) L, R are closest to the index M ,
 are verified.
5. Consider the new set of amplitudes $B_n(t)$

$$B_n(\Delta t) = \begin{cases} \frac{\hat{B}_n(\Delta t)}{A}, & L \leq n \leq R \\ 0, & \text{otherwise} \end{cases}$$

where

$$A = \left[\sum_{n=L}^R |\hat{B}_n(\Delta t)|^2 \right]^{\frac{1}{2}}$$

6. Consider $B_n(\Delta t + T)$ which are the solution to equation (10) for the initial values given by $B_n(\Delta t)$ and the time interval of integration equal to T . Verify that the mean square deviation

$$\sum_n [|B_n(\Delta t + T) - B_n(\Delta t)]^2, \quad \Delta t \ll T$$

is less than the accuracy level Err accepted. In case it is not met, set

$$\tilde{B}_n = B_n(t = 0)$$

else exit.

7. Return to step 2.

In case of solitons with large support, or long wavelengths, much larger than the spacing a , we can use the usual approach and look for solitons of the form (13), that is

$$Y(x, t) = e^{i(qna - \omega t)} \psi(na - vt)$$

On substituting $B_n(t)$ given above in equation (10), we obtain the two standard equations for the imaginary and the real parts of $B_n(t)$. In the long wavelengths limit, the imaginary one results in the equation for the velocity of soliton, which in our notation reads:

$$v = 2a \cdot \omega_P \cdot \sin(a \cdot q).$$

The real part gives a nonlinear functional equation for the amplitude ψ , which can be solved by the familiar Newton method.

It is important that, for long wavelengths, the RF-algorithm brings about the same results as the Newton method indicated above.

References

- [1] J.D. Watson and F.H.C. Crick, *Nature* **171**, 737 (1953).
- [2] W. Saenger, *Principles of Nucleic Acid Structure*, Springer-Verlag, New York (1984).
- [3] F.H.C. Crick and J.D. Watson, *Brookhaven Symp. Biol.* No. 8 (1956).
- [4] P.O. Löwdin, *Rev.Mod.Phys.* **35**, 724 - 732 (1963).
- [5] F.H.C. Crick, *J.Mol. Biol.*, **19**, 548 (1966).
- [6] M.D. Topal and J.R. Fresco, *Nature* **263**, 285 - 289 (1976).
- [7] Auerbach Ch., *Mutation Research*, London, John Wiley and Sons, (1976).
- [8] V.I. Poltev, M.V. Kosevic, V.S. Shelkovskii, V.A. Pashinskaja, E.X. Gon-sales, A.V. Tepluxin, and G.G. Malenkov, *Mol.Biology (Russian)*, **29**, 376 (1995).
- [9] H. Robinson, Yi-Gui Gao, Cornelia Bauer, Christopher Roberts, Christo-pher Switzer, and Andrew H.-J Wang, *Biochemistry* **37**, 10897 - 10905 (1998).
- [10] H. Kamiya and H. Kasai, *FEBS Lett.*, **391**, 113 - 116 (1996).
- [11] H. Kamiya and H. Kasai, *Biochemistry*, **36**, 11125 - 11130 (1997).
- [12] H. Kamiya and H. Kasai, *J.Biol.Chem.*, **270**, 2595 - 2600 (1995).
- [13] C. Switzer, S.E. Moroney, and S.A. Benner, *J.Am.Chem.Soc.*, **111**, 8322 - 8323 (1989).
- [14] Wu Suen, T.G. Spiro, L.C. Sowers, and J.R. Fresco, *Proc.Natl.Acad.Sci. USA* **96**, 4500 - 4505 (1999).
- [15] C. Switzer, S.E. Moroney, and S.A. Benner, *Biochemistry*, **32**, 10489 - 10496 (1993).
- [16] R. Geracitano and F. Persico, *Physiol.Chem. and Physcs*, **3**, 361 - 370 (1971).
- [17] C.A. Hunter, *J.Mol.Biol.* **230**, 1025 - 1054 (1993).
- [18] C.A. Hunter and J.K.M. Sanders, *J.Amer.Chem.Soc.* **112**, 5525 - 5537 (1990).
- [19] A.S. Davydov, *Sov.Phys. Usp.* **251**, 898 (1982).

- [20] P. Nelson, Proc.Natl.Acad.Sci. USA **96**, 14342 - 14347 (1999).
- [21] L.F. Liu and J.C. Wang Proc.Natl.Acad.Sci. USA **84**, 7024 - 7027 (1987).
- [22] C. Levinthal and H. Crane, Proc.Natl.Acad.Sci. USA **42**, 436 - 438 (1956).
- [23] M.Wang, M.J. Schnitzer, H. Yin, R. Landick, J. Gelles and S. Block, Science **282**, 902 - 907 (1998).
- [24] T.Dauxois, M.Peyrard, and A.R. Bishop, Phys.Rev. **E47**, R44 - R47 (1993).
- [25] V.L. Golo, E.I. Kats, and M. Peyrard, Pisma ZhETF **73**, 225 - 229 (2001).
- [26] V.L. Golo, E.I. Kats and Yu.M. Yevdokimov, Pisma ZhETF **70**, 766 - 770 (1999).
- [27] M. Bruant, D. Flatters, R. Lavery, and D. Genest, Biophys. J. **77**, 2366 - 2376 (1999).
- [28] E.B.Starikov, Phys.Rep. **284**, 1 - 89 (1997).
- [29] A.C. Scott, Phys.Rev. **A26**, 578 (1982).
- [30] A.C. Scott, Phys.Reports. **217**, 1 - 67 (1992).
- [31] S. Flach and C.R. Willis, Phys. Reports **295**, 181 - 264 (1998).
- [32] N. Bodor, M.J.S. Dewar, and A.J. Hagert, J.Amer.Che.Soc. **92**, 2929 (1970).
- [33] J.L.Leroy, K.Gehring, A.Kettani, and M.Guéron, Biochemistry, **32**, 6019 (1993).

Figure Captions

Fig.1

Schematic structure of the double helix of DNA.

Fig.2

Amino/imino and keto/enol forms of purine and pyrimidine.

Fig.3

Thymine-Adenine and Cytosine-Guanine pairing.

Fig.4

Pairing of cytosine, normal form, and adenine, imino form.

Fig.5

Pairing of thymine, enol form, and adenine, imino form.

Fig.6

Uracil-uracil pairing.

Fig.7

Pairing of adenine-(brom-uracil) and guanine-(brom-uracil).

Fig.8

Typical moving soliton for $W = 0.75$, $\Lambda = 0.001$, velocity 1325.28 base pairs per *msec*, the period of time spent 0.533 *msec*. The solid line shows $|A_n|^2$, and the thin lines indicate the real and the imaginary part of the amplitude A_n .

Fig.9

Breather, or still soliton. Typical moving soliton for $W = 10$, $\Lambda = 0.5$, velocity 0 base pairs per *msec*, the period of time spent 0.501 *msec*. The solid line shows $|A_n|^2$, and the thin lines indicate the real and the imaginary part of the amplitude A_n .

Fig.10

Radiation emitted from the motionless central peak during the period of time 0.018, for $W = 5$ and $\Lambda = 0.5$; the velocity of side waves 1833.3 base pairs/*msec*, distance traveled 33 base pairs. The solid line shows $|A_n|^2$, and the thin lines indicate the real and the imaginary part of the amplitude A_n .

Fig.11

Moving soliton for $W = 0.75$, $\Lambda = 0.075$, velocity 1335.46 base pairs per *msec*, the period of time spent 0.530 *msec*, distance travelled 707 base pairs. The solid line shows $|A_n|^2$, and the thin lines indicate the real and the imaginary part of

the amplitude A_n .

Fig.12

Moving soliton for $W = 2$, $\Lambda = 0.1$, velocity 851.2 base pairs per *msec*, the period of time spent 0.577 *msec*, distance travelled 491 base pairs. The solid line shows $|A_n|^2$, and the thin lines indicate the real and the imaginary part of the amplitude A_n . The values of W , Λ are close to the borderline (see Fig.17), dividing the region of stable solitons from the unstable ones.

Fig.13

Partial self-focusing of an initial low amplitude distribution on a peak for a period of time 0.002 *msec*, for $W = 1$, $\Lambda = 0.5$.

Fig.14

Pairing of thymine and 2'-Deoxyisoguanosine.

Fig.15

Filter algorithm for finding solitons. The solid line indicates the part of the excitation to be preserved, and the thin line the does the part to be cut off, the dashed line means the precision.

Fig.16 (a)-(d)

Sets of W and ν , which allow for soliton solutions, at fixed Λ :

- (a) for $\Lambda = 0$
- (b) for $\Lambda = 0.1$
- (c) for $\Lambda = 0.15$
- (d) for $\Lambda = 0.2$

The solid line shows still solitons, or breathers, and the shaded area indicates moving solitons. We take into account only solitons of size less than 100 base pairs.

Fig. 1

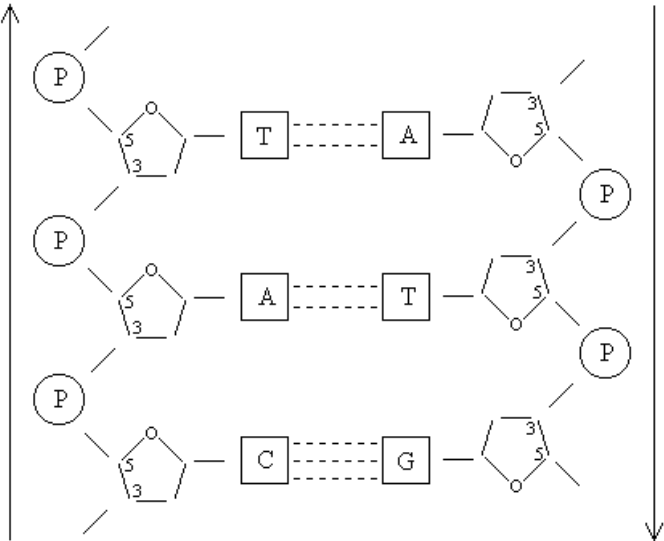


Fig. 2

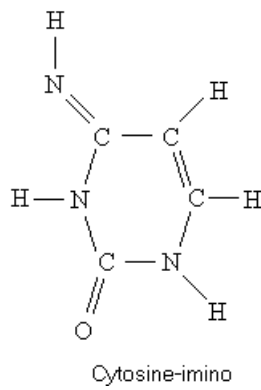
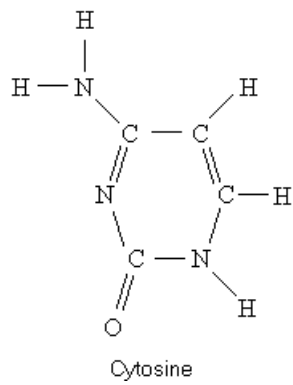
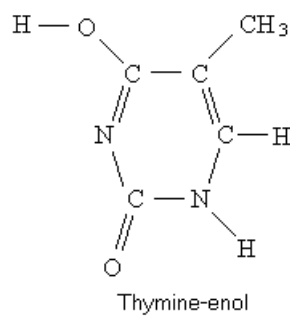
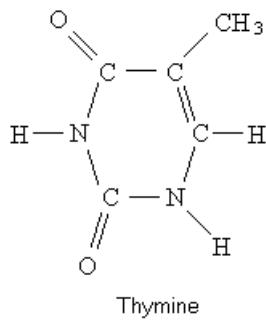
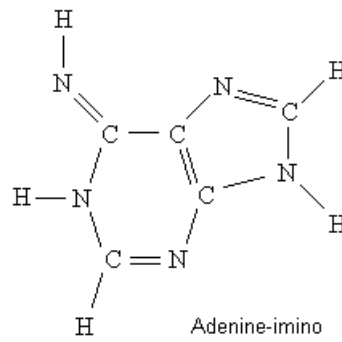
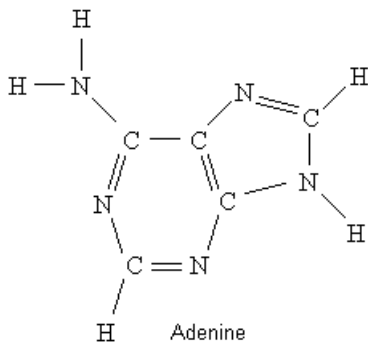
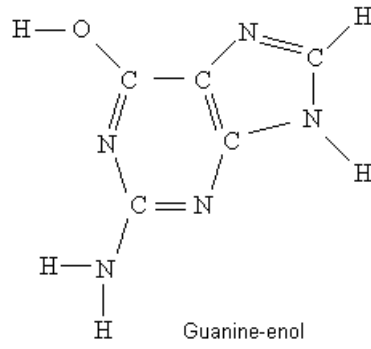
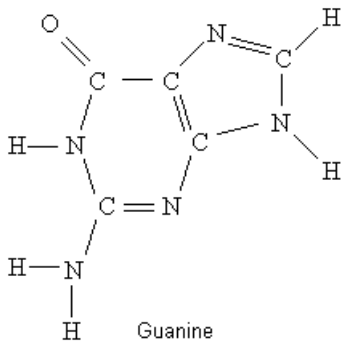


Fig. 3

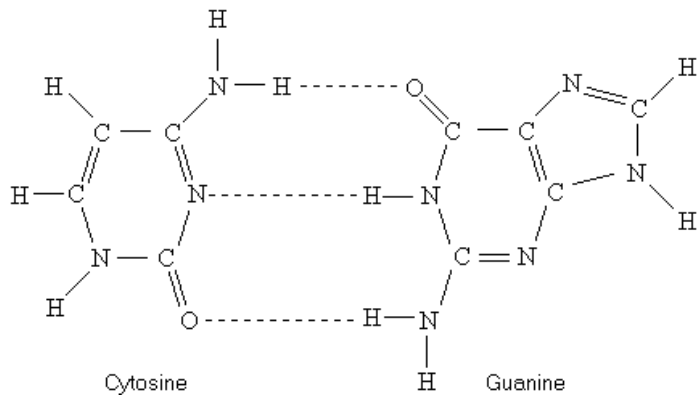
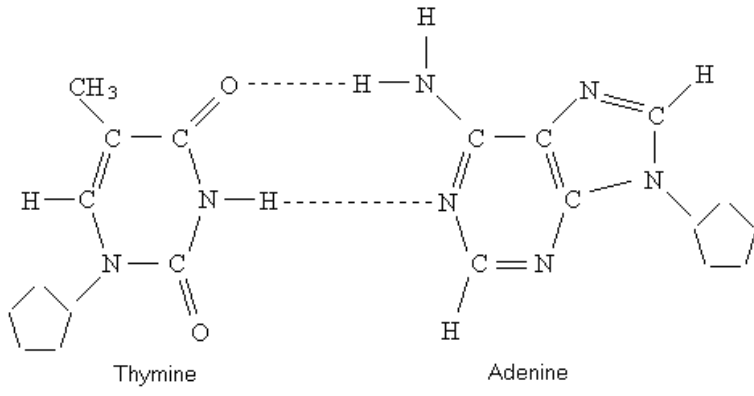


Fig. 4

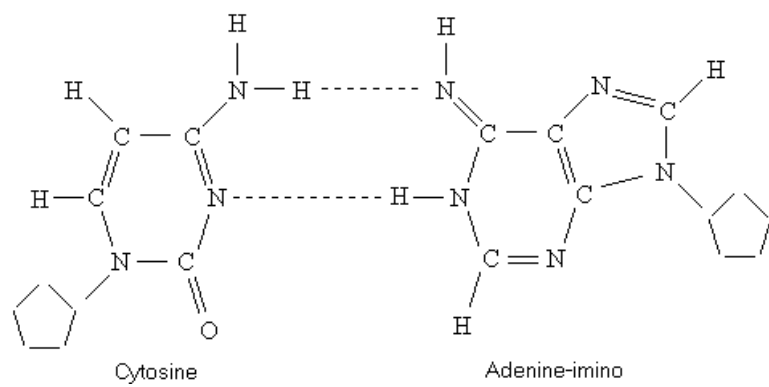


Fig. 5

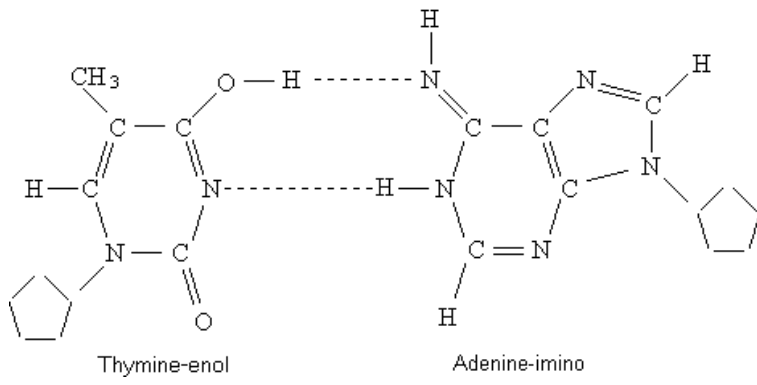


Fig. 6

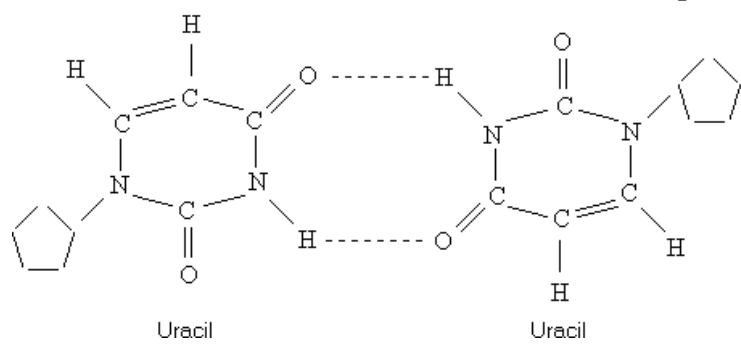


Fig. 7

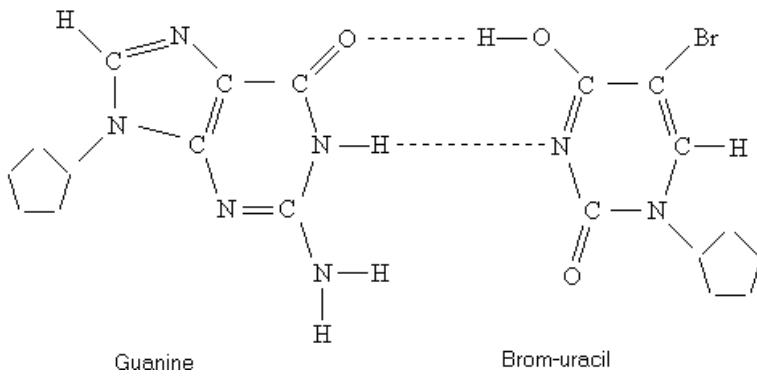
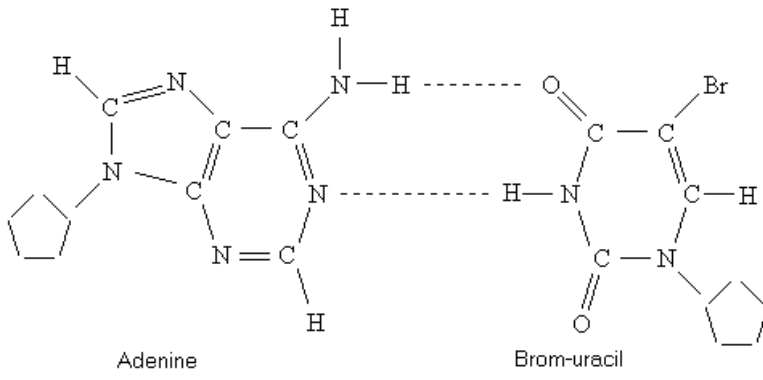


Fig. 8

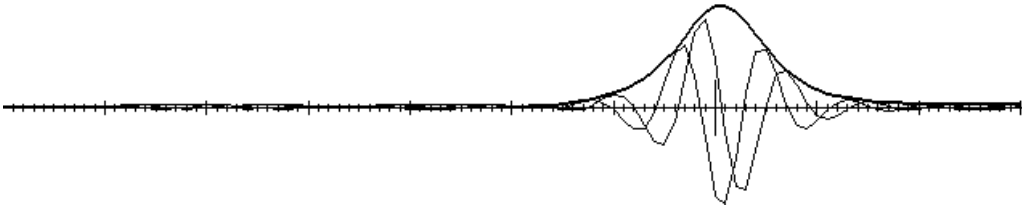


Fig. 9

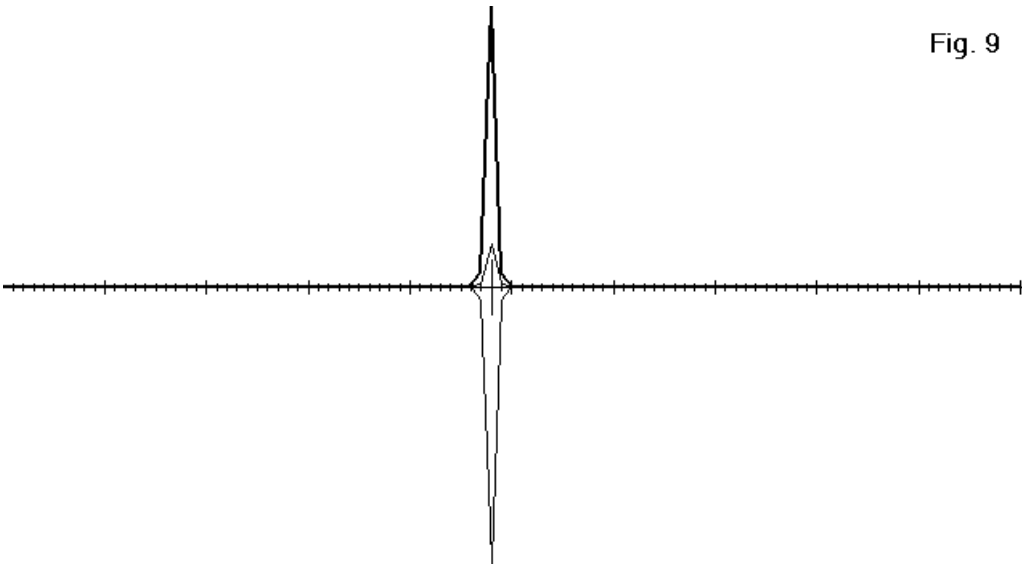


Fig. 10

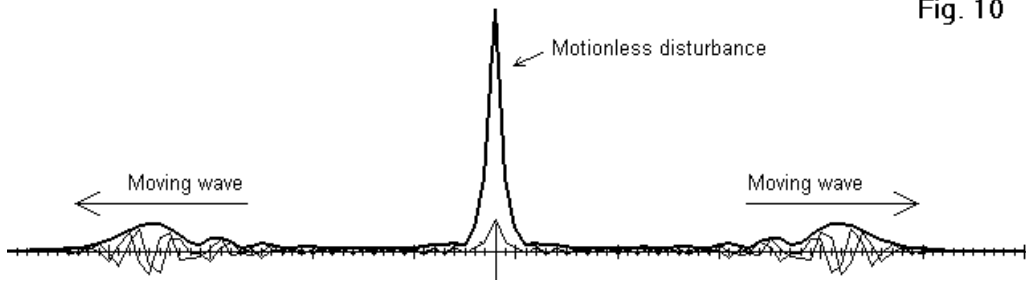


Fig. 11

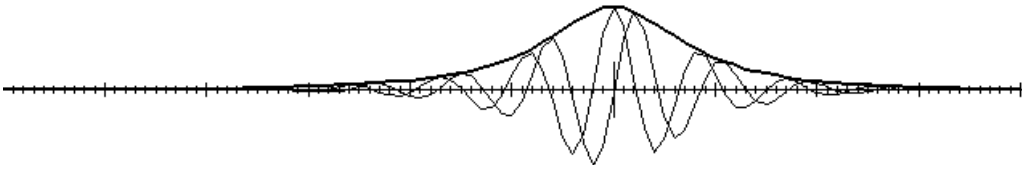


Fig. 12

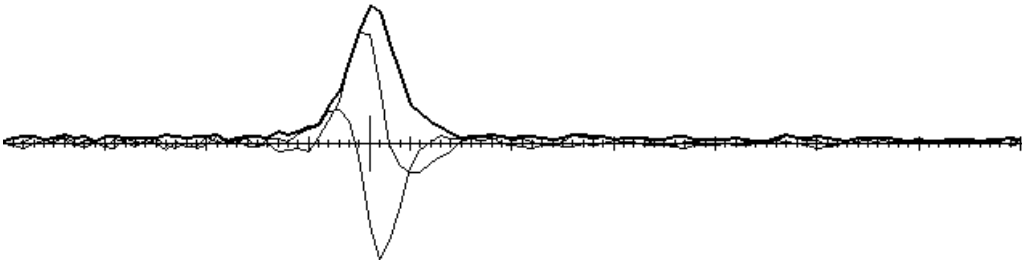


Fig. 13

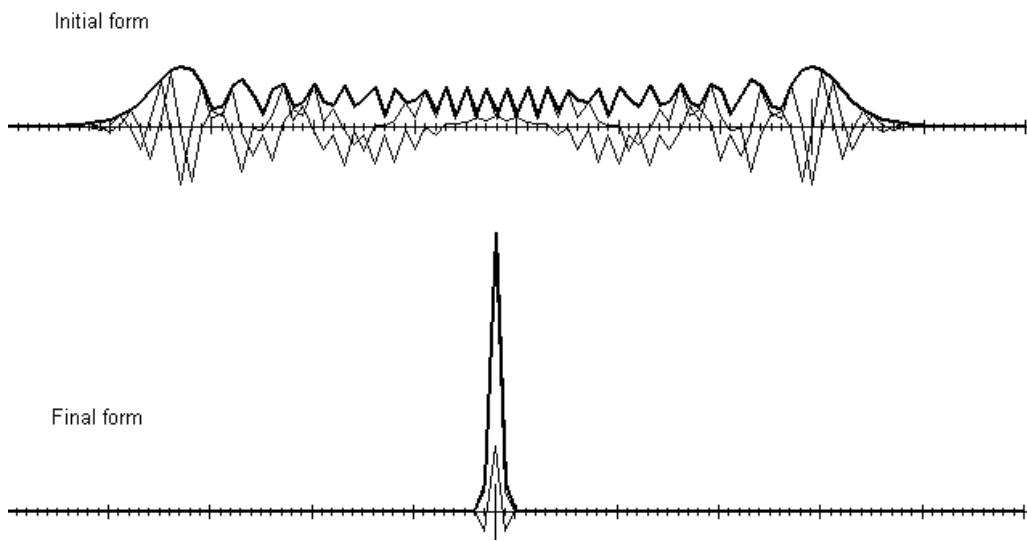


Fig. 14

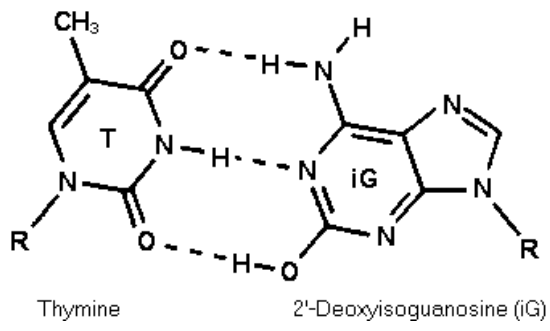
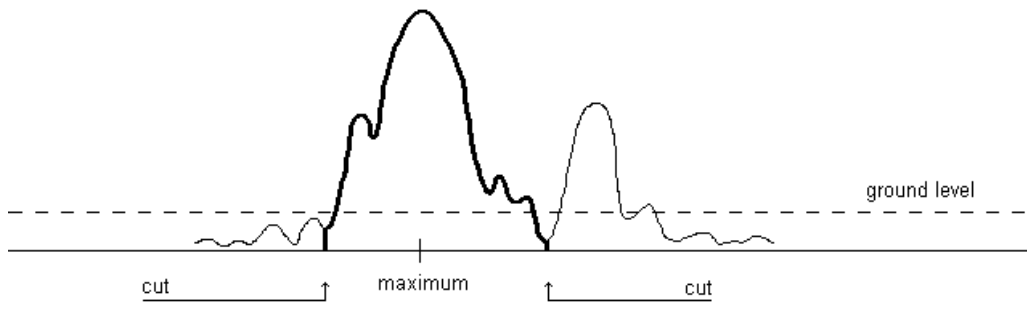


Fig. 15



Filter algorithm

Fig. 16 (a)

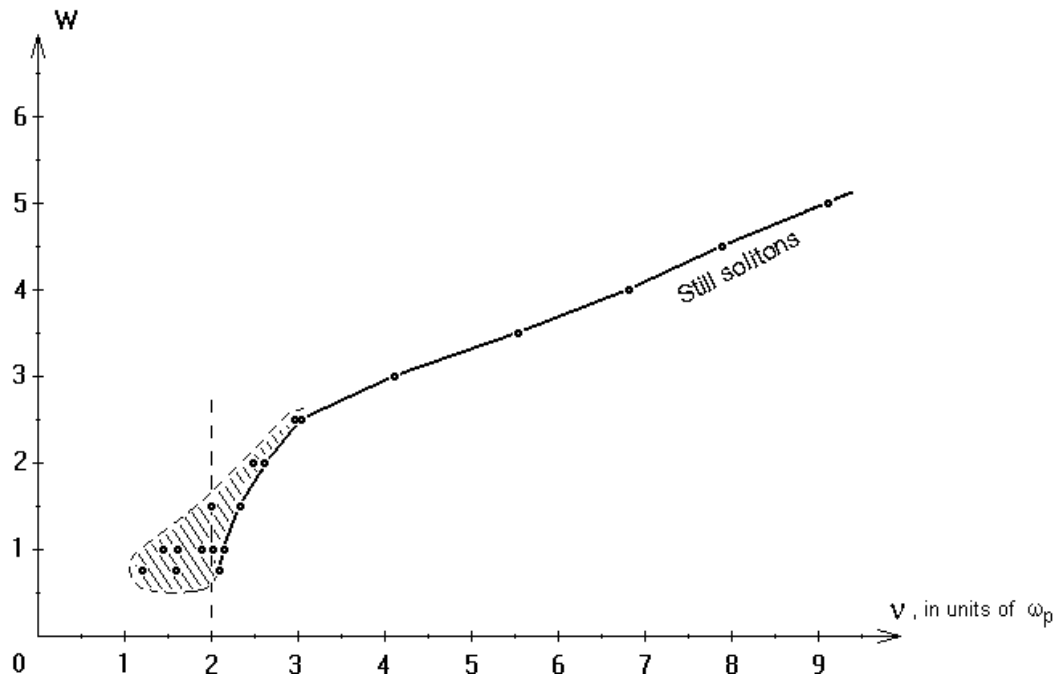


Fig. 16 (b)

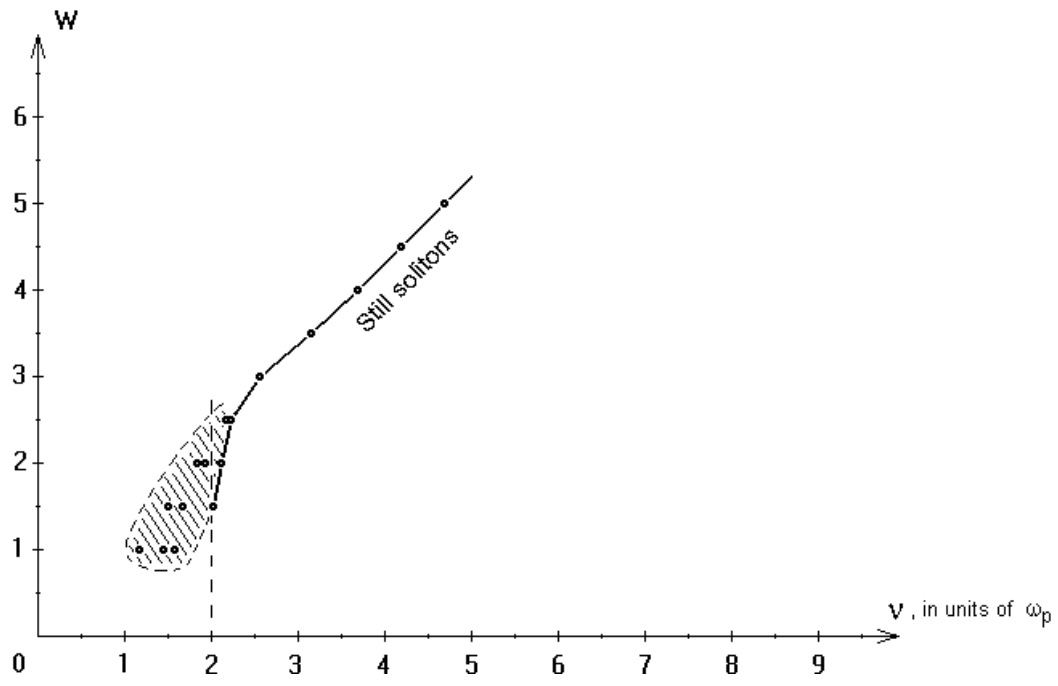


Fig. 16 (c)

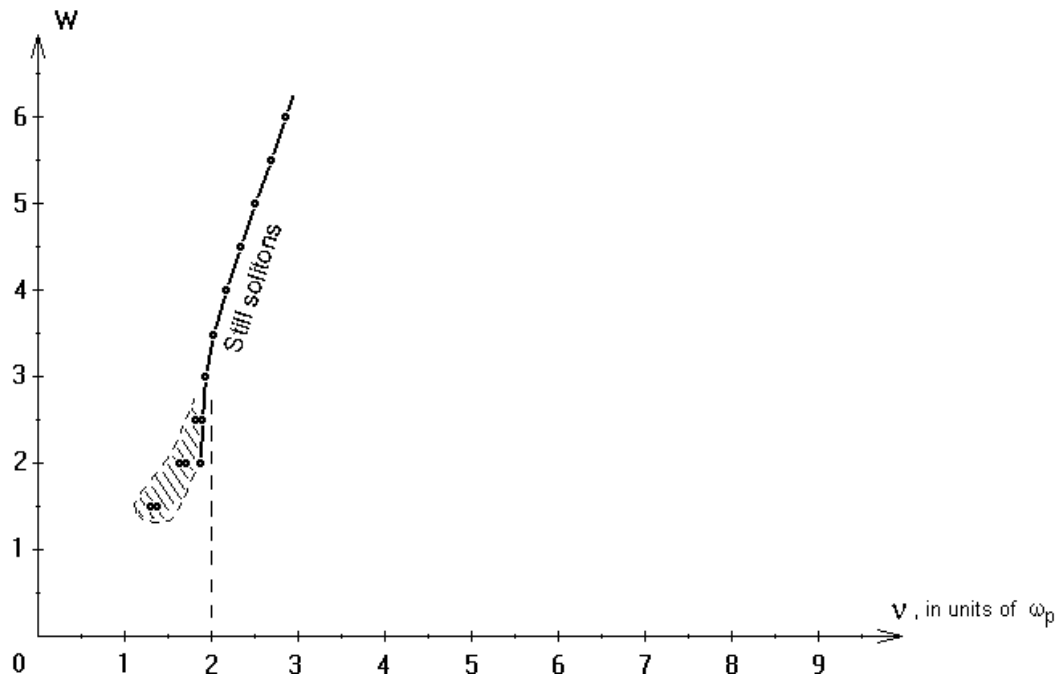


Fig. 16 (d)

